5.4 Flow through a pure contraction.

If the bottom remains horizontal (h^*=constant), and the flow is choked only by contractions in the width of the rectangular channel, a new type of control condition can come into play. Solutions can still be represented in the Armi (1986) Froude number plane and Figure 5.4.1a shows an example with $|Q_r|$=1. The thinner contours continue to represent constant $|Q_2^*| / \left[(z_T^* - h^*)^{3/2} g'^{1/2} w^* \right]$, except that w^* rather than h^* is considered as varying from one contour to the next. Decreasing values of w^* generally lead one away from the origin. The form (5.3.1) of the energy equation is no longer convenient for constructing solution curves since w^* appears as a scale factor. A more helpful form

$$\frac{\frac{1}{2}F_2^{4/3} - \frac{1}{2}Q_r^{2/3}F_1^{4/3} + F_2^{-2/3}}{Q_r^{2/3}F_1^{-2/3} + F_2^{-2/3}} = \frac{\Delta B}{g' z_T^*} = d_{2\infty} \qquad (5.4.1)$$

is obtained by setting h^*=0 and using (5.3.2) to eliminate w^* from (5.3.1). The internal energy is now represented by $d_{2\infty}$ which, in view of (5.2.10), is the interface elevation in the hypothetical wide, quiescent basin. The thick curves in Figure 5.4.1a are contours of constant $d_{2\infty}$. Exchange flows and unidirectional flows having the same values of $|Q_r|$ and $|Q_2^*|$ are again represented by the same diagram, though differences in stability and jump-forming capabilities render some combinations unrealizable. In contrast to the case of variable topography, both layers feel the geometric variations directly. There is now a symmetry between the behavior of the upper and lower layers. For the solutions curves shown in the figure, all of which have $|Q_r|$=1 , this means that a solution with a particular $d_{2\infty}$ has a counter part in which the layers are reversed. That is, F_1^2 and F_2^2 are interchanged and $d_{2\infty}$ is replaced by 1- $d_{2\infty}$. More generally, for a given Q_r there is a comparable solution with flow rate ratio $1/Q_r$ in which the two layers are interchanged (see Exercise 2.)

a. Submaximal flow from a wide basin.

Figure 5.4.1a represents solutions for which the volume flow rates in the two layers have equal magnitude. There is a family of constant energy curves that emanate from the origin ($F_1^2 = F_2^2 = 0$) and represent flows originating from an infinitely wide, quiescent basin. Let us first restrict attention to unidirectional flow. All of the curves beginning at the origin intersect the critical diagonal, indicating the presence of a critical section for sufficiently small minimum width w_m^*. For all but one of these curves, the contours of constant width make grazing contact with the solution curves along the critical diagonal. Critical flow for these solutions occurs at the narrowest section. Continuation past this section leads to supercritical flow, possibly with a hydraulic jump. If the upper layer thickness is greater than the lower layer thickness in the basin

($d_{2\infty}$<0.5) then the lower layer is thinned and accelerated, and the upper layer is thickened and decelerated, through the contraction. An example is given by the curve *afm* of Figure 5.4.1b. The opposite is true when $d_{2\infty}$>0.5 as indicated by curve *ain*. The behavior of the thinner layer in each case is similar to single layer flow through a contraction.

b. Self-similar flow.

Of the Figure 5.4.1a curves originating from the origin, there is one that does not cross the critical diagonal at a point of minimum width. This 'similarity' solution is given by the straight line $F_1^2=F_2^2$ and corresponds to equal basin layer thicknesses ($d_{2\infty}$=0.5). Since $|Q_r| = 1$this solution is characterized by equal layer depth and speed at each section. If the flow is unidirectional then v_1*=v_2* and the fluid behaves as if it were homogeneous, entirely bereft of internal dynamics. Beginning at the origin, one can trace a solution from the upstream basin through the narrowest section. For relatively large values of the narrowest width (in particular, q_2<0.25) the flow will remain subcritical and will resemble something like the trace *ala* in Figure 5.4.1b. As w_m* is decreased (and the corresponding q_2 increased), the trace may just reach the critical diagonal and will therefore become critical at the narrowest section, remaining subcritical elsewhere. A further decrease in w_m* causes the solution to cross the critical diagonal and become supercritical. Where the diagonal is crossed (point *b*) the solution curve is normal to the curves of constant q_2. In other words, critical flow occurs not at the minimum width but at a point of diminishing width: $\partial w^*/\partial y^* < 0$. The existence of this *virtual control* is consistent with the regularity condition (5.2.17) and the fact that $v_1{}^{*2}(y_c) - v_2{}^{*2}(y_c^*) = 0$. Downstream of the virtual control the flow becomes supercritical and remains so as the narrowest section, say *c* in Figure 5.4.1b, is passed. In principle, the solution then retreats back along the same line towards the origin, passing through another virtual control. The idealized path is something like *abcba* in Figure 5.4.1b. In reality, a slight amount of dissipation will cause the flow to move off of the supercritical portion of the similarity solution and onto one of the supercritical solutions (with $d_{2\infty}\neq 0.5$). The downstream flow may eventually be returned to a subcritical state by a hydraulic jump. The circuit traced is therefore something like *abcdefa* or *abcghia*, the choice influenced by downstream conditions.

A similar barotropic solution exists for each value of Q_r (Exercise 4). Since the velocities in each layer are equal, Q_1* and Q_2* are each proportional to the net transport Q* (=Q_1* +Q_2*). We proved in Section 5.2 that the latter remains independent of time if it is so far upstream and thus Q_1* and Q_2* must also remain independent of time. Thus the similarity solution is not subject to blocking as the result of upstream influence. The minimum width may be made arbitrarily small without effecting the layer transports. In graphical terms, the act of making w_m* small, and q_2 large, simply forces the solution flow at the narrowest section (point *c*) to extend farther from the origin. There is no nothing that forces Q_1* or Q_2* to change.

c. Laboratory examples of unidirectional flow.

Armi (1986) has produced examples of these solutions in a laboratory channel with a width contraction (Figure 5.4.2). The two layers are pumped from right to left at fixed values of Q_1* and Q_2* such that Q_r=1. The channel narrows to a minimum width midway through and widens again at the left end. Here, there is nothing like a quiescent reservoir and the flow is varied by changing the net transport Q* (=Q_1* +Q_2*) and by altering the downstream conditions. For smaller values of Q*, Armi finds hydraulically controlled flows that resemble the solutions with unequal layer depths ($d_{2\infty}$<0.5 or $d_{2\infty}$>0.5) as described above. Examples are given in Figures 5.4.2a,b and the corresponding solution traces are something like *afm* or *ain* in Figure 5.4.1b. In both cases the flow is subcritical until it reaches the narrowest section, where it undergoes a transition to supercritical flow. The particular solution arising from a specified Q* (=2Q_2* in the experiment) is predicted by calculating the value of q_2 (=Q_2 * /(z_T *$^{3/2}$ $g'^{1/2}w_m$*)) at the narrowest section and finding the intersection of the corresponding q_2=constant curve with the critical diagonal in Figure 5.4.1a. For q_2<.25 there will be two such intersections and therefore one must choose between two solutions, one having $d_{2\infty}$<0.5 and the other $d_{2\infty}$>0.5. In the experiment, the choice is forced by downstream conditions that influence the initial evolution by which the steady flow is set up.

If Q* is increased, the value of q_2 at the narrowest section increases, forcing the intersection with the critical diagonal to move closer to the midpoint F_1^2= F_2^2=1/2. The value of $d_{2\infty}$ for the corresponding solutions approaches 0.5, meaning that the layer depths become equal. At the value q_2=0.25 the similarity solution is obtained and the layer depths become equal, at least in principle, at all points along the channel. A further increase in Q* forces a self-similar flow with a virtual control. As discussed above, the predicted flow enters the channel in a subcritical state and passes through a virtual control, becoming supercritical, on its way to the narrowest section. It continues to flow at a supercritical speed through the narrows. A laboratory realization is shown in Figure 5.4.2c. The flow wanders a bit from it's predicted self-similar state downstream of the narrows, probably due to frictional effects. In principle, Q* can be increased without limit, not surprising when one considers that the flow is behaving as if the density were uniform.

A virtual control clearly operates in a different way, and has different implications for the upstream flow, than a standard narrows or sill control. For example, the flows shown in frames *a* and *b* of the figure experience upstream effects, manifested in the interface height, in response to changes in the minimum width w_m*. The same in not true of the flow with the virtual control (frame *c*), which is supercritical through the narrows. As discussed above, changes in the value of w_m* therefore no upstream effect whatsoever. Instead, the virtual control acts to maintain the barotropic character of the flow. Its appearance coincides with the disappearance of shear between the two layers. Through the regularity condition, it requires that v_1*=v_2*, and thus establishes a shear-free state at the position of the control. Since the sidewall forcing acts equally on each layer, the shear-free state extends upstream and downstream from the position of the

virtual control. In essence, the virtual control has driven all internal dynamics out of the flow, which now acts like a single, homogeneous layer.

d. Lock exchange flow

Under conditions of pure exchange (Q_r=-1) similar versions of most of the above solutions can be found. One that is not observed is the exchange version of the similarity solution, which now has $v_1^* = -v_2^*$ and is unstable upon entry into the supercritical region. However another solution comes into play: the one indicated by the energy curve $d_{2\infty}$=0.5 that makes grazing contact with the critical diagonal in Figures 5.4.1a or b. This solution can be imagined to occur between two wide basins, one in which the top layer is very thin and the other in which the lower layer is very thin. This situation is difficult to realize when the flow is unidirectional (see Exercise 3), however it can readily be established for an exchange flow. The traditional method of doing so is to perform a 'lock exchange' experiment of the type suggested in Figure 5.3.2, but with a pure width contraction in place of an obstacle. Removal of a barrier placed at the contraction allows the fluids to move in opposite directions, displacing each other above and below, eventually resulting in a steady solution of the type just described. The flow is critical at the narrowest section, where *both* c_-^* and c_+^* vanish, and becomes supercritical on either side. Hydraulic jumps typically arise in these supercritical extensions, so that the complete solution circuit is something like *aijbkfa* in Figure 5.4.1b. The direction of wave propagation in the supercritical regions is always away from the narrowest section and thus the flow there is insulated from small disturbances generated in the neighboring basins.

Asymmetric exchange solutions corresponding to solutions like *ain* or *afm* in Figure 5.4.1b can also be established in the laboratory. One approach (e.g. Lane-Serff, et al. 2000) to perform a 'partial' lock exchange experiment in which the barrier holding back the denser fluid extends from the bottom only part way up to the rigid lid. The dense fluid is filled only to the top of the barrier and the barrier itself is positioned at the channel contraction. After release, the steady exchange flow that is established has a lower layer that is thinner overall than the upper layer. The flow state corresponds to one of the solutions with $d_{2\infty}$<0.5, of which *afm* is an example, in Figure 5.4.1b. Cases with $d_{2\infty}$<0.5 may be established by positioning the initial barrier to extend from the rigid lid partially down to the bottom and filling the less dense fluid to this lower level. The complete range of exchange states is sketched in Figure 5.4.3.

The 'full' lock exchange solution achieves the maximum value of q_2 (=0.25) of any of the realizable exchange solutions. This solution therefore reaches the maximal flux

$$Q_2^* = .25 g'^{1/2} w_m^* D_s^{3/2}, \qquad (5.4.2)$$

for fixed minimum width w_m*, over all possible internal energy levels. The formula follows from use of the definition of q_2 along with its observed value, or simply by

setting $|Q_r|=1$ in (5.3.4). This solution is characterized by a double hydraulic control in the sense that both internal waves are frozen at the narrows. Stommel and Farmer (1952) identified this state and verified it experimentally.[1] Their analysis and their later (1953) application to estuary dynamics (Section 4.5) deserve special mention in the annals of hydraulics as one of the first applications of hydraulic theory to oceanographically relevant flows. Both layers are engaged: the upper layer being more so in one reservoir, the second in the other, and both being active at the narrowest section. The submaximal solutions ($d_{2\infty}\neq 0.5$) are characterized by having only one wave frozen at the narrowest section, by having a smaller Q_2* for the same w_m*, D_s and g', and by being dominated by the dynamics of one of the layers.

It is possible to devise a number of experiments demonstrating how maximal flow is obtained as a limiting case of the submaximal flows. For example, one might carry out a series of lock exchange solutions in which the initial barrier extends only partially through the depth. One reservoir is filled to the top with the lighter fluid. The other is filled to the top of the barrier with the denser fluid with the less dense fluid lying above. If this partial barrier is low enough, the exchange flow set up by its removal will be submaximal. Increasing the barrier height sufficiently will eventually lead to the maximal solution. A similar set of experiments could be made by pumping the fluids in opposite directions and gradually increasing the pumping rates. The sequence of exchange solutions that one might encounter is shown in Figure 5.4.3.

e. Unequal layer fluxes.

Froude number diagrams for $|Q_r|\neq 1$ show similar features with a few twists. The case $|Q_r|=0.5$ is shown in Figure 5.4.4a. Under conditions of exchange (Q_r=-0.5), the flow contains a barotropic component Q_1*+Q_2*, here equal to Q_1*/2. A similarity solution with the virtual control exists and corresponds to the straight contour with $d_{2\infty}$=2/3. For general $|Q_r|$, the corresponding value of $d_{2\infty}$ is given by $(|Q_r|+1)^{-1}$ and the contour itself by $|Q_r|F_1^2 = F_2^2$ (see Exercise 4). However, the former 'lock exchange' solution, which occurs along the curved energy contour with $d_{2\infty}$=2/3, now has two intersections with the critical diagonal. The lower right intersection corresponds to a virtual control and the upper left intersection to a narrows control. It can be shown that the virtual control lies on the side of the narrows from which the barotropic component of the flow originates. Also, there is a group of solutions with $d_{2\infty}$ slightly greater than 2/3 that intersect the critical diagonal twice and that go off into supercritical space at either end. Since both F_1^2 and F_2^2 go to infinity following the right-hand branch of these curves, the corresponding solutions cannot be smoothly connected to an infinitely wide reservoir.

[1] However, it was not recognized as the maximal limit of a continuum of other controlled solutions until the work of Armi (1986) and Farmer and Armi (1986).

The physical separation of the two control section in the presence of barotropic flow was first recognized by Wood (1970), who also coined the term 'virtual control'. In an exchange flow, the virtual control clearly operates in a different manner that its unidirectional counterpart. The compatibility condition only requires that the flow speeds in the two layers be equal. In the limiting case of zero barotropic flow studied by Stommel and Farmer (1952) the virtual control is hidden by the fact that the two controls occur together.

If the flow is unidirectional and originates from a wide reservoir, the range of possible behavior can be illustrated, as before, by imagining a series of experiments in which the value of q_2 ($=Q_2 */(z_T *^{3/2} g'^{1/2} w_m *)$) is gradually increased by increasing Q_2*. We continue to assume that the flow is critical at the narrows. Beginning along a solution curve for which $d_{2\infty}>2/3$, we move through a succession of flows with relatively deep lower layers. These solutions have upper layers that are relatively active and that are accelerated through the contraction. However, the transport in the lower layer is twice that in the upper layer and the dynamics of this layer are more easily brought into play. As Q_2* is raised the similarity solution is realized when $d_{2\infty}$ reaches the value 2/3. Here the lower layer depth remains twice the upper layer depth along the entire solution curve. For further increases in Q_2* the solution remains along the similarity curve and develops a virtual control upstream of the narrows. As before, the flow becomes supercritical through the narrowest section and, in the expanding section of channel, tends to wander off of the $d_{2\infty}=2/3$ curve. Possible outcomes with weakly dissipative jumps are illustrated by the paths *abefgha* or *abeijha* in Figure 5.4.4b.

If instead we begin with a solution for which $d_{2\infty}<2/3$, the approach to the similarity solution is just slightly different. We move through a series of solutions like *ahm* in which the lower layer is most active. As Q_2* is raised, a solution traced by the curve *abcd* is approached from the left. The subcritical flow from the reservoir is nearly self-similar as it enters the contracting section and nearly passes through a virtual control there. The solution now lies just to the left of point *b* in Figure 5.4.4b. The solution then veers away from the similarity curve and passes through a narrows control (point c*)*, after which it becomes supercritical. A further increase in Q_2* gives rise to the similarity solution with a virtual control.

Under conditions of exchange, a similarly modified sequence of solutions exists. As Q_2 is increased from low values the limiting form is no longer the similarity solution (which is again unstable) but rather the full lock exchange solution. This solution has supercritical flow extending into the two reservoirs and subcritical flow between the two controls. A hydraulic jump or some other source of dissipation is required to join the supercritical flows to the quiescent reservoirs. An example is given by the circuit *alkbcdha* in Figure 5.4.4b. A procedure for obtaining a weir formula for this case is explored in Exercise 8.

Exercises

1) By free hand, sketch the qualitative features of the solutions corresponding to the following circuits:

a) *afm* (Figure 5.4.1b)
b) *ain* (Figure 5.4.1b)
c) *abcba* (Figure 5.4.1b)
d) *jbk* (Figure 5.4.1b)
e) *aijbkfa* (Figure 5.4.1b)
f) *kbcd* (Figure 5.4.4b)
g) *alkbcdha* (Figure 5.4.4b)

The sketches should be the style of the Figure 5.3.1b insets, with control sections and stretches of subcritical and supercritical flow labeled.

2) For flow through a contraction with constant h^*, show that for each Q_r there is another solution with reciprocal flow rate ratio $(1/Q_r)$ in which the two layers are interchanged.

3) Consider the following flows, each of which has at least one critical section. Remark on the stability of the hydraulic transition at the critical section(s) in each case. (Refer to the shock-forming instability, not Kelvin-Helmholtz instability.)

(a) The solution *kjk* in Figure 5.4.1b.

(b) A solution of the type *abcd* in Figure 5.4.1a, with the lower layer entering the deep basin and the upper layer exiting the basin.

(c) The 'lock exchange' solution with Q_r=0.5. In other words, the solution with both a virtual and narrows control lying along the $d_{1\infty}$=.667 curve in Figure 5.4.1a, but now with unidirectional flow.

4) Prove that a barotropic (v_1=v_2) solution exists for arbitrary Q_r. Show that the solution is represented in the Froude number plane by $|Q_r|F_1^2 = F_2^2$ and that the corresponding value of $d_{2\infty}$ is $(1+|Q_r|)^{-1}$.

5) Show that where the similarity solution of Exercise (4) intersects the critical diagonal, a second solution with the same $d_{2\infty}$ must exist.

6) The two solutions implied in Exercise 5 must both satisfy (5.4.1) with $d_{1\infty} = (1+|Q_r|)^{-1}$. With this setting show, in fact, that (5.4.1) can be written in the form

$$\left(F_2^{2/3} - |Q_r^{1/3}|F_1^{2/3}\right)\left[\tfrac{1}{2}F_1^{2/3}F_2^{2/3}\left(1+|Q_r|\right)\left(F_2^{2/3}+|Q_r^{1/3}|F_1^{2/3}\right) - Q_r^{2/3}\right] = 0 . \qquad (5.4.4)$$

Show that satisfaction of this relation by equating the leading expression to zero gives the barotropic (similarity) solution. Setting the longer, expression to zero gives the pure lock exchange solution.

7) For Q_r=-1, show using equation (5.4.4) that the curve defining the lock exchange solution is identical to the curve (5.2.11) defining the long-wave stability threshold. (Hint: note that Q_r is negative.) This result was first shown by Lawrence (1993).

8) If the definition of q_2 is applied at the narrows, an implicit 'weir' formula is obtained:

$$Q_2^* = (q_2)_{narrows}\, w^*\, g'^{1/2} D_s^{\,3/2}.$$

Here $(q_2)_{narrows}$ is the value of q_2 corresponding to point *c* in Figure 5.4.4b, or the equivalent figure for the value of Q_r in question. Using a result obtained in Exercise 6, write out a procedure for calculating $(q_2)_{narrows}$ in terms of Q_r for the maximal lock exchange solution (eg. *kbcd* of Figure 5.4.4b). (The algebra may be too complex to obtain a closed form solution.)

Figure Captions

Figure 5.4.1a The Froude number plane for flow through a pure contraction with $|Q_r|$=1. Solutions must lie along the thick curves, which have constant $d_{2\infty}$. The thin curves are of constant q_2 and are the same as in Figure 5.3.1a, but now the larger values of this parameter are associated with narrower widths. (From Armi,1986)

Figure 5.4.1b Examples of solutions for the previous figure, as described in the text.

Figure 5.4.2 Side views of unidirectional, two-layer flows through a contraction. Frames (a) and (b) show flows with a control section at the narrowest section, which lies approximately at the numeral '2'. Frame (c) shows a self-similar flow with a virtual control. At the upstream (right) entrance the layer depths and velocities are equal and continue to be so as the channel converges and the narrowest section is passed. The virtual control occurs somewhere to the right of the narrowest section but is not distinguished by any visual property of the interface. A small amount of mixing is observed in the downstream end of the channel. (From photos appearing in Armi, 1986).

Figure 5.4.3. A sequence of steady solutions for two-layer exchange through a pure contraction, as described in the text. (Based a figure in Armi and Farmer, 1986)

Figure 5.4.4a Froude number plane for flow through a pure contraction with $|Q_r|$=0.5. (Based on a figure in Armi and Farmer, 1986**.)**

Figure 5.4.4b Examples of solution traces based on the curves shown in (a).

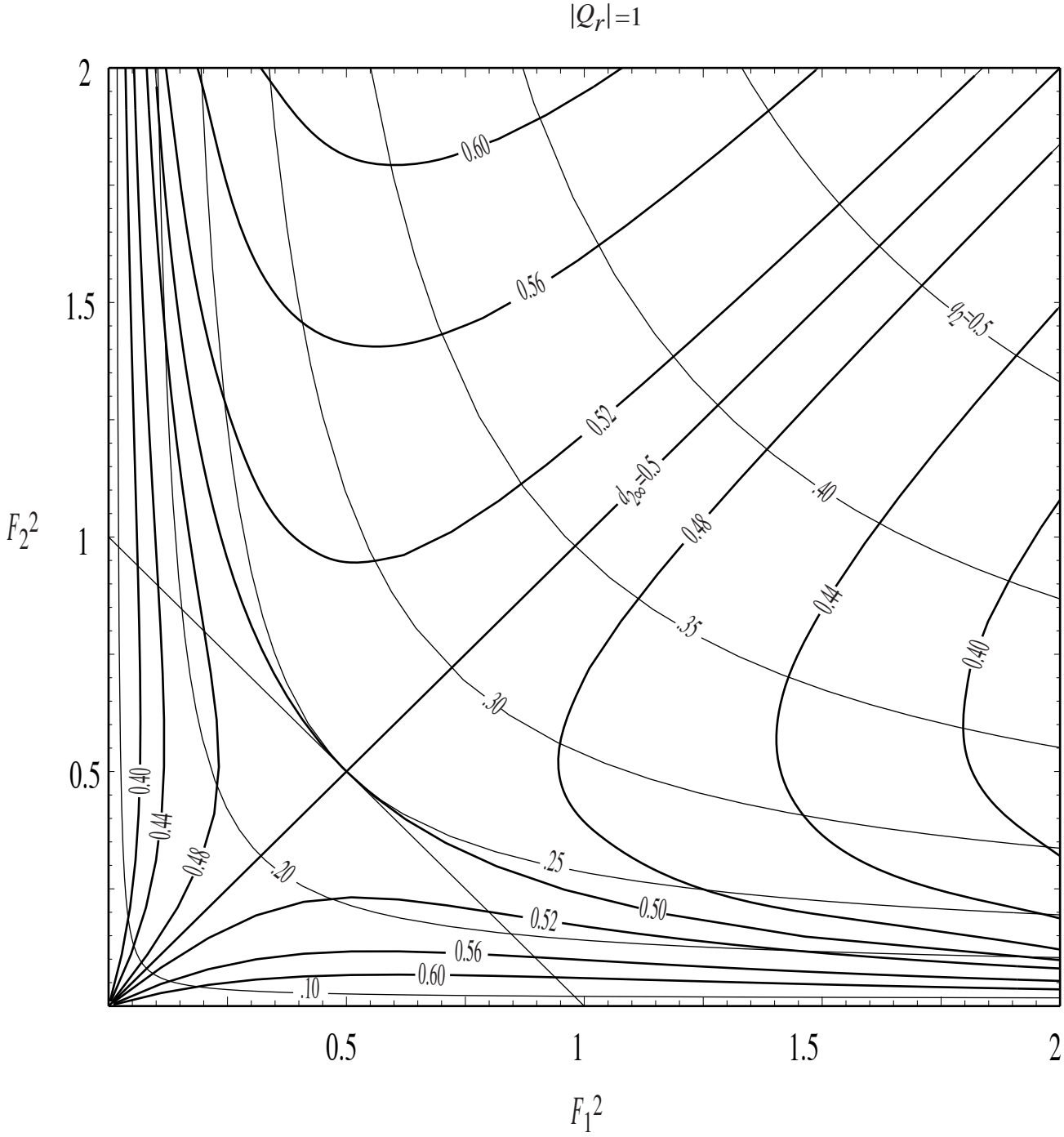
$|Q_r|=1$
2
1.5
1
0.5
F_2^2
0.5
1
1.5
2
F_1^2
0.60
0.56
0.52
$\theta_2=0.5$
$\theta_{2\infty}=0.5$
.40
0.48
0.44
.35
0.40
.30
0.40
0.44
0.48
.20
.25
0.50
0.52
0.56
0.60
.10

Fig. 5.4.1a

$|Q_r|=1$

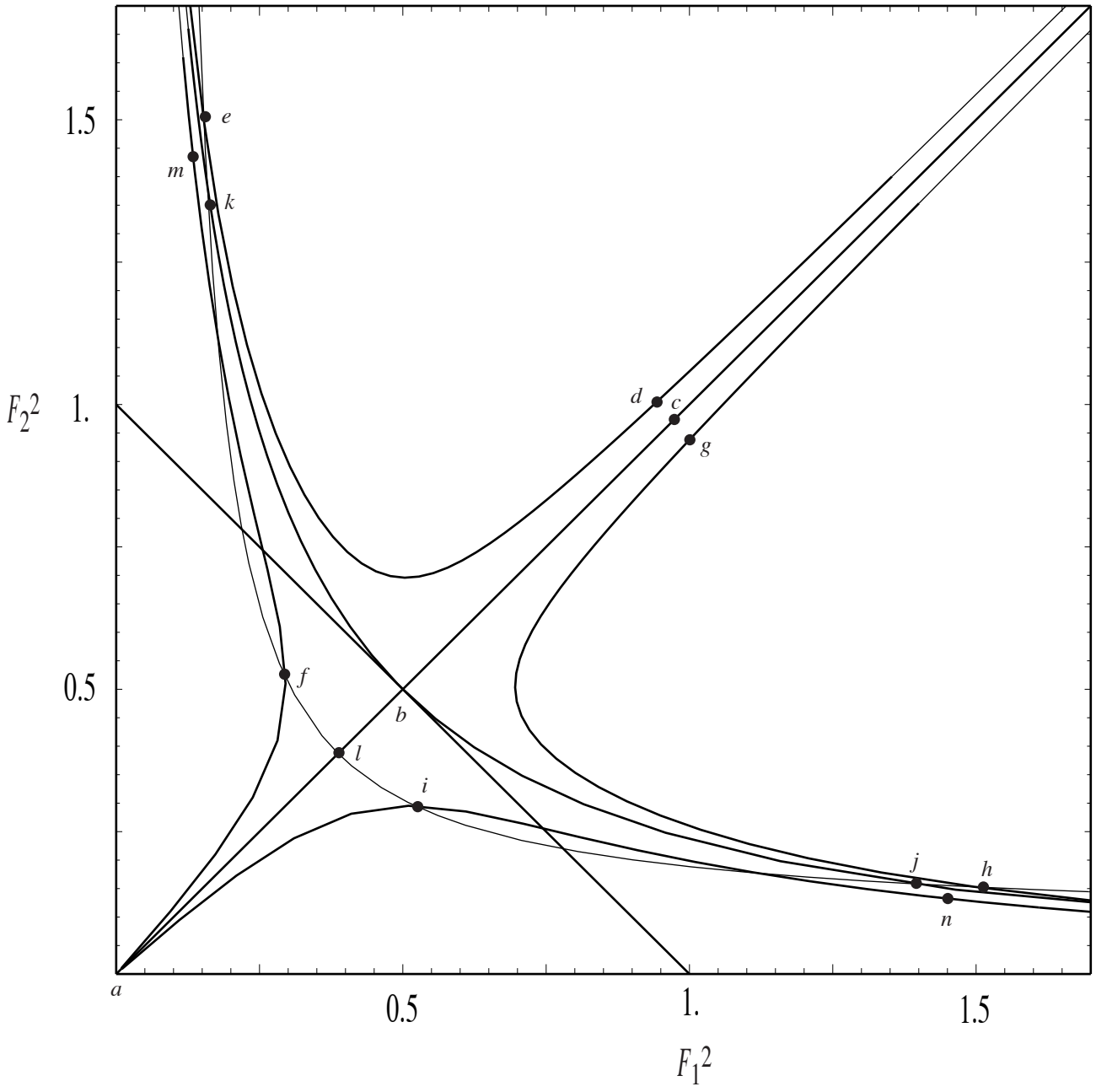

Fig. 5.4.1b

narrowest section

(a)

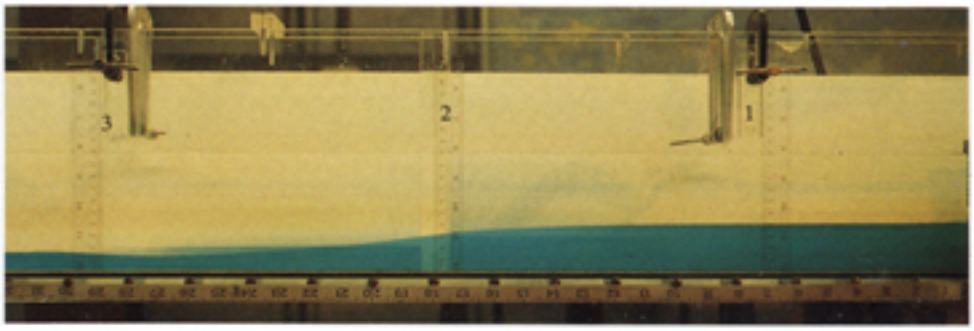

(b)

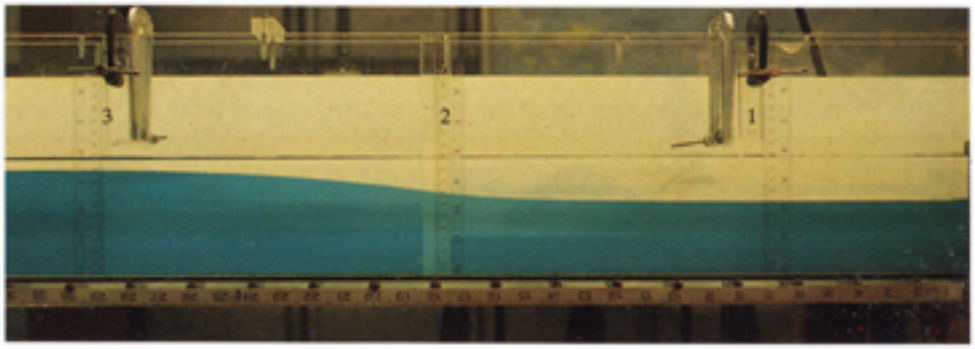

(c)

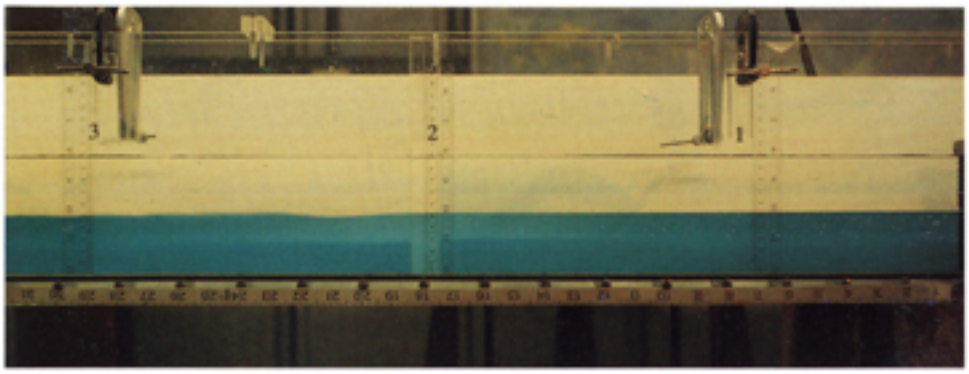

Figure 5.4.2

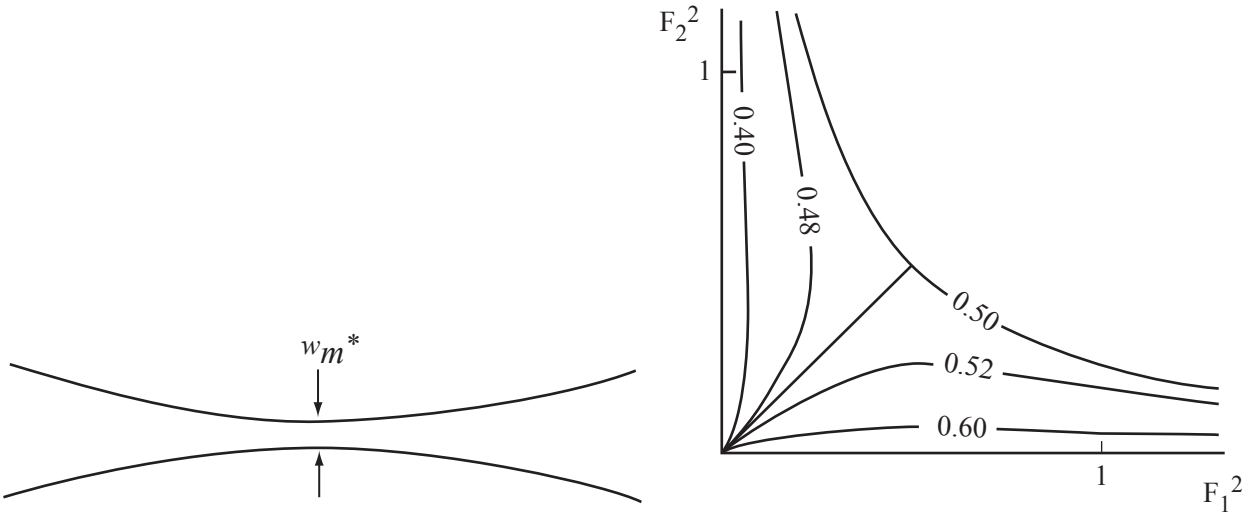

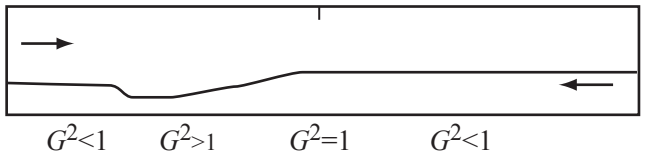

$d_{2\infty}=0.40$

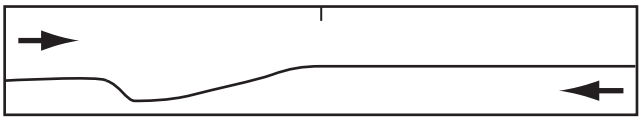

$d_{2\infty}=0.48$

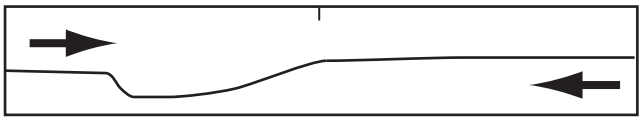

$d_{2\infty}=0.50^-$

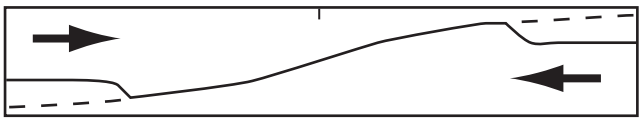

$d_{2\infty}=0.50$

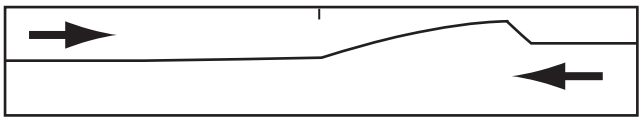

$d_{2\infty}=0.50^+$

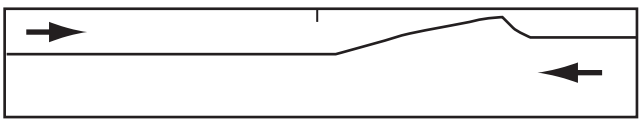

$d_{2\infty}=0.52$

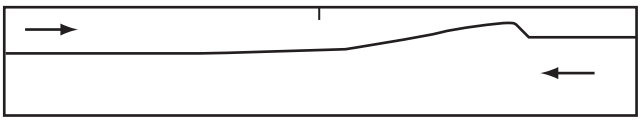

$d_{2\infty}=0.60$

Figure 5.4.3

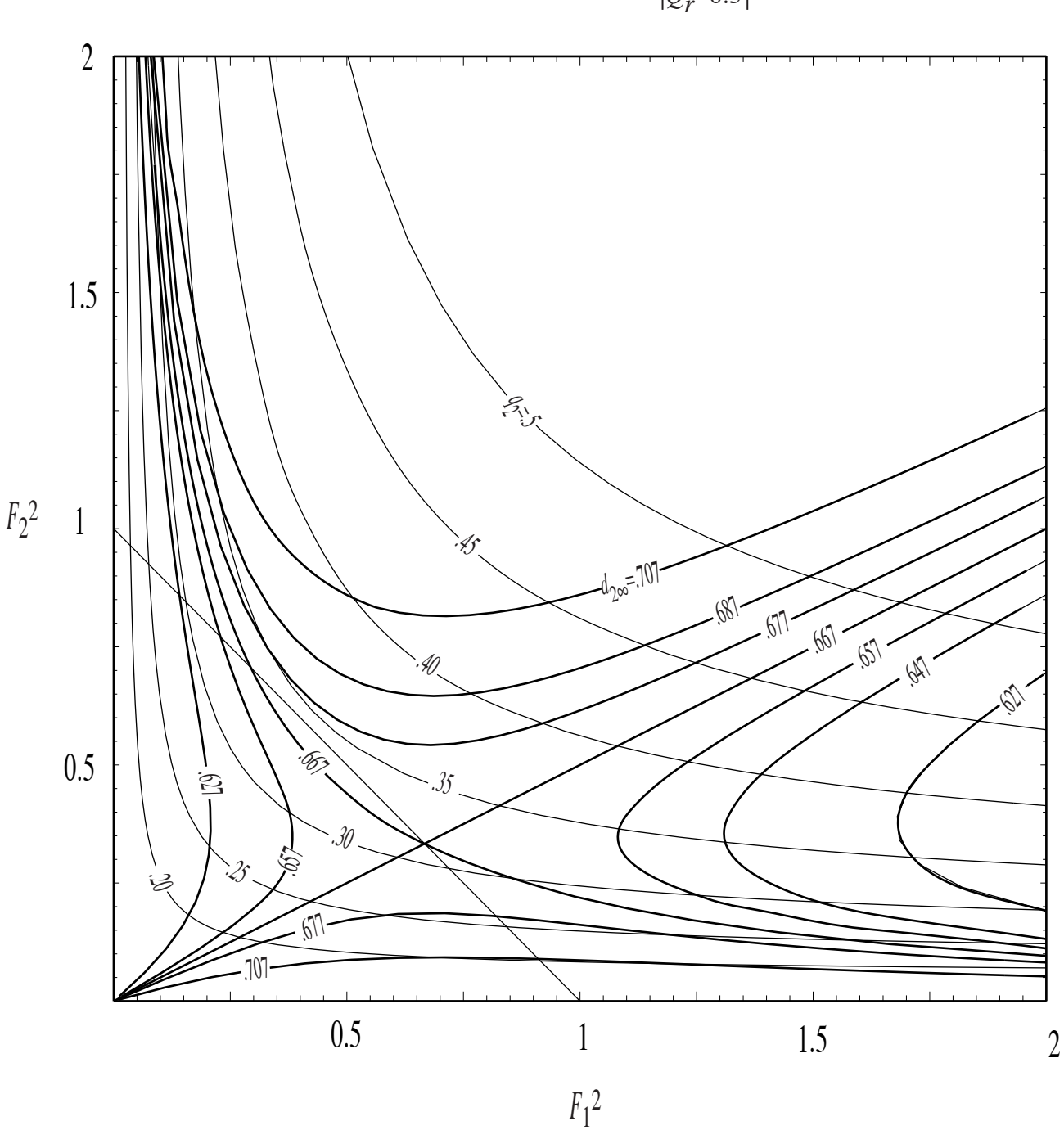
$|Q_r$=0.5|
2
1.5
1
0.5
F_2^2
0.5
1
1.5
2
F_1^2
.45
.40
.35
.30
.25
.20
$d_{2\infty}$=.707
.687
.677
.667
.657
.647
.627
.667
.627
.657
.677
.707

Fig. 5.4.4a

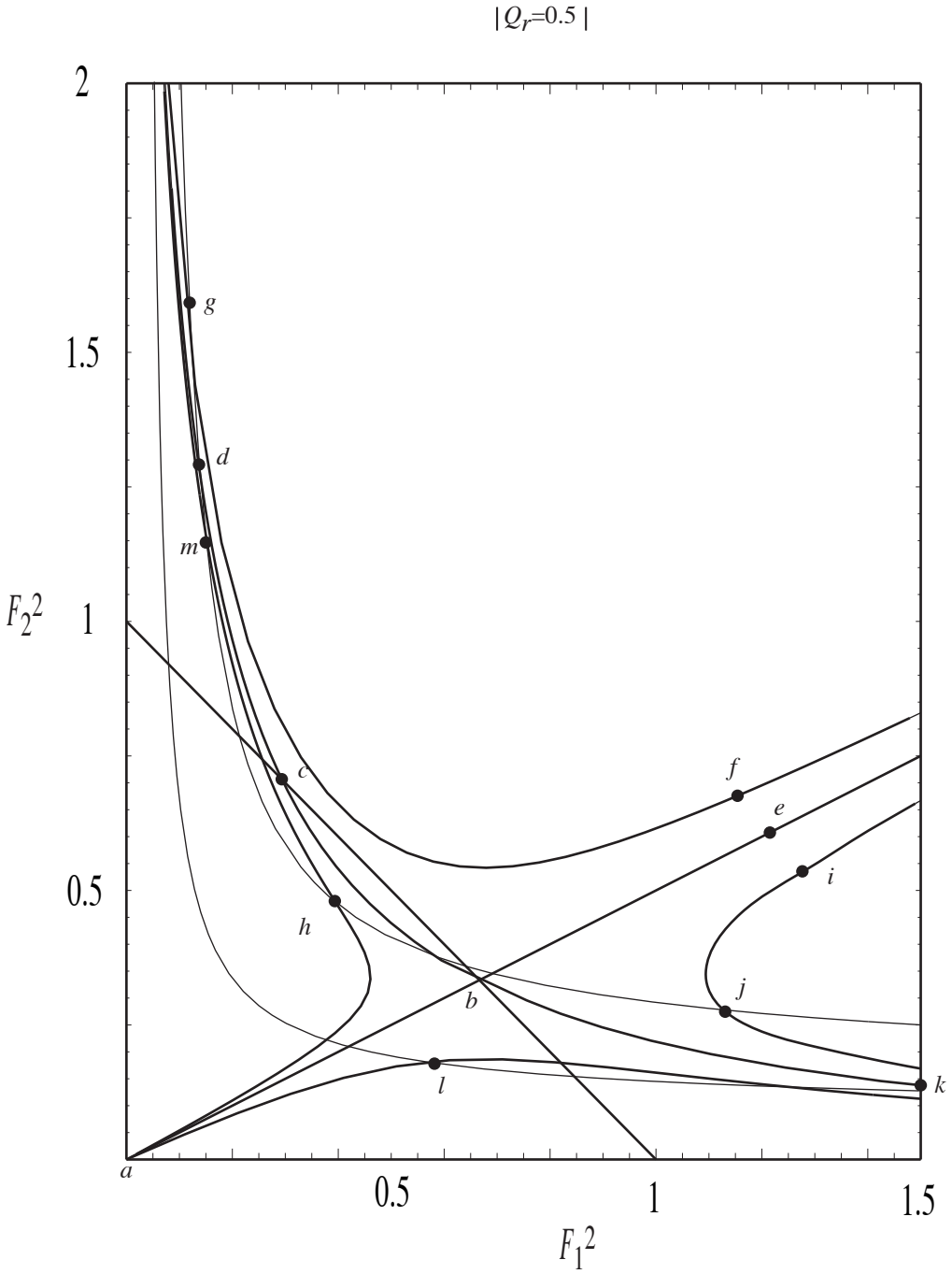

Fig. 5.4.4b